frontiers | Frontiers in Ecology and Evolution

TYPE Original Research
PUBLISHED 29 June 2023
DOI 10.3389/fevo.2023.1175220

OPEN ACCESS

EDITED BY
Lin Zhang,
Hubei University of Chinese Medicine, China

REVIEWED BY
Jingguang Wei,
South China Agricultural University, China
Biswajit Maiti,
Nitte University, India
Simin Chai,
Southern Marine Science and Engineering Guangdong Laboratory (Guangzhou), China

*CORRESPONDENCE
Zhengfei Wang
wangzf01@yctu.edu.cn

†These authors have contributed equally to this work

RECEIVED 27 February 2023
ACCEPTED 13 June 2023
PUBLISHED 29 June 2023

CITATION
Chen L, Tang D, Hua Y, Wang X, Li Y and Wang Z (2023) Molecular characterization, adaptive evolution, and expression analysis of the *Toll-like receptor* gene family in *Fenneropenaeus chinensis*. *Front. Ecol. Evol.* 11:1175220. doi: 10.3389/fevo.2023.1175220

Molecular characterization, adaptive evolution, and expression analysis of the *Toll-like receptor* gene family in *Fenneropenaeus chinensis*

Lulu Chen[1,2†], Dan Tang[1,2,3†], Yuyan Hua[1,2], Xinyu Wang[1,2], Yanxuan Li[1,2] and Zhengfei Wang[1,2*]

[1]Jiangsu Key Laboratory for Bioresources of Saline Soils, Jiangsu Synthetic Innovation Center for Coastal Bio-Agriculture, School of Wetlands, Yancheng Teachers University, Yancheng, Jiangsu, China, [2]Jiangsu Provincial Key Laboratory of Coastal Wetland Bioresources and Environmental Protection, School of Wetlands, Yancheng Teachers University, Yancheng, Jiangsu, China, [3]Senior High School Teaching Department, Shazhou Middle School, Zhangjiagang, Jiangsu, China

Global warming is a challenge to animal health because of the increased environmental temperature, with subsequent induction of immune suppression and increased susceptibility to disease during summer. The Toll-like receptor (TLR) family is an essential pattern recognition receptor (PRR) that initiates the innate immune response by sensing conserved molecular patterns of pathogens. However, research on the *TLR* gene family in decapod crustaceans has been conducted sporadically, without systematic naming, and the relationship between pathogen immunity adaptation and adaptive evolution of immune-related genes is unclear. In this study, various *TLR* gene sequences in decapod crustaceans were collected, and the unified name of *Fenneropenaeus chinensis* was confirmed using sequence alignment. Structural characteristics and evolutionary analyses of *TLR* genes in decapod crustaceans were performed, and ten *FcTLR* genes were identified in *F. chinensis*. Protein domain analysis revealed that FcTLR proteins contain 4–25 LRR domains used to recognize different pathogens. Selection pressure analysis revealed that *TLR1* and *TLR9* were subjected to positive selection pressure in decapod crustaceans, which may be related to their resistance to environmental changes. Furthermore, the expression of ten *TLR* genes was detected in *F. chinensis* following white spot syndrome virus (WSSV) infection. The results demonstrated that *FcTLR1*, *FcTLR7*, and *FcTLR9* responded positively, which was also consistent with the results of the protein domain and selection pressure analyses. This study provides new insights into the immune response and adaptive evolution of *TLRs* in decapod crustaceans to prevent environmental damage, such as pathogens and high temperature.

KEYWORDS

***Fenneropenaeus chinensis*, innate immunity, TLR, WSSV infection, adaptive evolution, expression analysis**

1 Introduction

Global warming is a huge challenge to animal health, causing a decline in animal production and the suppression of immune function (Li et al., 2021). Reports on climate change predicted that the global temperature may rise between 1.4°C and 4.8°C by the end of this century (IPCC, 2014; Savitha et al., 2021). Shrimps and crabs can be found in almost any ecosystem, including shallow coral reefs and hydrothermal vents in the ocean, as well as freshwater and terrestrial habitats (Ma et al., 2019; Wang et al., 2021). As a kind of ectotherm, species of Decapoda are more susceptible to changes in body temperature than endotherms with changes in environmental temperature (Chen et al., 2020). Temperature is considered as a major factor that regulates the development and response of the immune system in decapod crustaceans especially aquaculture organisms (Miest et al., 2019). During periods of elevated temperatures in summer, aquaculture organisms enter a rapid growth period, particularly with respect to the growth and reproduction of microorganisms. Due to the decrease in oxygen content and deterioration of aquaculture environment, pathogen infection is the main disease at this stage.

The innate immunity of decapod crustaceans serves as the main barrier against infections by many pathogens. Innate immunity relies on unique pattern recognition receptors (PRRs) that recognize the unique pathogen-associated molecular patterns (PAMPs) in external pathogenic microorganisms (Habib and Zhang, 2020). After receiving the signal, it is transmitted to the cell through a series of cascade reactions to regulate the transcription and expression of immune effector factors, which are quickly induced to prevent foreign substances from causing harm to the body (Hughes and Piontkivska, 2008). The Toll-like receptor (TLR) family is an essential PRR family that initiates the innate immune response by sensing the conserved molecular patterns of pathogens. They are the first line of defense against pathogen invasion and play key roles in inflammation, immune cell regulation, survival, and proliferation (Habib and Zhang, 2020; Wan et al., 2022).

TLRs are transmembrane proteins that are involved in signal transduction at the surface of the cell membrane. They are remarkably conserved in the evolutionary process and have three specific domains: interleukin-1 receptor (TIR), transmembrane domain structure, and leucine-rich repeats (LRR) (Wan et al., 2022). TLRs can be roughly divided into two categories based on their location and respective PAMP ligands within the cell. On the surface of cells, a class of TLRs (TLR1, TLR2, TLR4, TLR5, TLR6, and TLR11) mainly recognizes microbial membrane components, such as lipids, proteins, and lipoproteins (Kawai and Akira, 2010; Xing et al., 2017). Intracellular vesicles, such as the endoplasmic reticulum (ER), endosomes, lysosomes, and endolysosomes, contain other intracellular TLRs (TLR3, TLR7, TLR8, and TLR9) that mainly recognize nucleic acids of microorganisms or viruses, such as dsRNA, ssRNA, siRNA, shRNA, and viral DNA (Barton and Kagan, 2009; Li et al., 2019).

In 1980, TLRs were first discovered in *Drosophila melanogaster* embryos (Nusslein-Volhard et al., 1980), and homologous TLRs were found in mice and adult *D. melanogaster* in the 1990s (Chiang and Beachy, 1994; Hoshino et al., 1999). The immune response mechanism mediated by TLRs to recognize antigens invading the body has also been uncovered. Subsequently, 10 and 13 *TLRs* (*TLR1–13*) were found in vertebrates, such as humans and mice (Roach et al., 2005), whereas nine *TLRs* (*Toll1–9*) were identified in *D. melanogaster* (Ooi, 2001). Among aquatic organisms, many *TLRs* have been identified in fish, among which 27 *TLRs* have been found in *Cyprinus carpio* (Gong et al., 2017) and 16 *TLRs* in *Lateolabrax maculatus* (Fan et al., 2019). The number and function of *TLRs* vary greatly among fish species.

In decapod crustaceans, Li et al. (2018) discovered a relatively complete family of nine *TLRs* (*Toll1–9*) in *Litopenaeus vannamei* (Li et al., 2018). In a subsequent study by Habib et al. (2021), 11 *TLRs* in *L. vannamei* were identified through the genome-wide screening. Furthermore, *LvToll4* was a crucial receptor for sensing white spot syndrome virus (WSSV) and therefore activated the downstream pathway to induce the production of specific antimicrobial peptides (AMP) (Habib et al., 2021). Moreover, ten *TLRs* were identified in *Marsupenaeus japonicus* (Zheng et al., 2020), and seven *TLRs* were identified in *Procambarus clarkii* (Wan et al., 2022). However, only scattered genes have been cloned into other shrimp and crab species. For instance, five *TLRs* have been found in *P. clarkii* (Wang et al., 2015; Lan et al., 2016a; Lan et al., 2016b; Huang et al., 2017) and two in *M. japonicas* (Mekata et al., 2008). Three *TLRs* have been found in *Penaeus monodon* (Arts et al., 2007; Assavalapsakul and Panyim, 2012; Liu et al., 2018), two *TLRs* in *Macrobrachium rosenbergii* (Srisuk et al., 2014; Feng et al., 2016), two *TLRs* in *Scylla paramamosain* (Chen et al., 2018), and only one *TLR* in *F. chinensis* (Yang et al., 2008); however, the number and structure of *TLRs* are not completely understood.

WSSV is a common pathogen in aquatic organisms. Shrimp and crabs are highly infectious and have a very high mortality rate. It is considered the most serious threat to the aquaculture industry, leading to severe annual economic losses to the aquaculture industry. WSSV is a large enveloped double-stranded DNA (dsDNA) virus, which is highly pathogenic and especially virulent for prawns; hence, it is also known as prawn WSSV (Sun and Zhang, 2022). The interaction between WSSV and its shrimp host has received increasing attention, but the expression patterns of *TLR* and Toll-pathway-related genes involved in viral infection remain unclear. *Toll1*, *Toll2*, and *Toll3* were upregulated after WSSV attack in *L. vannamei* experiments, but their function in WSSV infection is poorly understood. During WSSV infection, the expression of antimicrobial peptides (AMPs) was induced by TLR proteins in *Cherax quadricarinatus* (Li et al., 2017), *P. clarkii* (Lan et al., 2016a; Lan et al., 2016b), and *M. rosenbergii* (Feng et al., 2016), suggesting that these AMPs may have antiviral effects. Furthermore, WSSV infection activated Toll pathway genes in *P. monodon*, implying that the entire Toll pathway plays a crucial role in the immune response during WSSV infection (Arts et al., 2007). Overall, some shrimp TLR proteins are involved in innate immune responses against viral infection; however, their antiviral function remains unknown, and their potential antiviral mechanisms require further investigation.

More than 90% of aquaculture production comes from Asia, including but not limited to China, Thailand, Bangladesh, and India (Bondad-Reantaso et al., 2005; Piamsomboon et al., 2016; Macusi et al., 2022). *Fenneropenaeus chinensis* is an important aquaculture shrimp in China, with endemic aquaculture species in the Yellow Sea and the Bohai Sea of China and the highest annual production of 200,000 tons (Gao et al., 2023). During 1988–1993, aquaculture production of prawns ranked first worldwide for several years. However, after the WSSV attack in 1993, the *F. chinensis* aquaculture industry suffered a huge blow, and its production and output value declined significantly. The Toll signaling pathway plays an important role in the resistance of shrimp to antigens, such as viruses. Therefore, it is essential to investigate the expression pattern of the *TLR* gene under WSSV stress in healthy shrimp and crab breeding, and it is also of great significance to further explore the functional differentiation of members of the *TLR* gene family and the responses of *TLR* genes under the long-term evolution pressure.

In this study, the *TLR* gene family was identified in *F. chinensis* at the genome scale, and a *TLR* gene tree was constructed using available *TLR* gene sequences from Decapoda in the NCBI genome database and transcriptome databases to better characterize these *FcTLR* genes. To elucidate the functional differentiation of *TLR* genes in *F. chinensis*, selective pressure analysis was employed to examine the evolutionary adaptation of *TLR* genes to the environment in the decapod crustaceans. Additionally, qRT-PCR was used to determine the relative expression level of crucial *TLR* genes in *F. chinensis* in response to WSSV infection.

2 Materials and methods

2.1 Experimental materials

F. chinensis for the WSSV infection experiment was obtained from the Huaguoshan Market in Lianyungang City, Jiangsu Province, China. Samples with a complete body, full vitality, and similar size were selected as test animals. The average body length of *F. chinensis* was nearly 120 mm, and the average weight was between 15 g and 20 g. The other species sequenced in the transcriptome were sampled from the Renmin Road Market and coastal beach of Yancheng City, Jiangsu Province, China.

2.2 Acquirement of sample data

The *TLR* genes analyzed in this study were extracted from five public genomic datasets (*Eriocheir sinensis*, *Portunus trituberculatus*, *Paralihodes platypus*, *L. vannamei*, and *F. chinensis*) from the NCBI database, and nine transcriptome datasets (*P. clarkii*, *Cardisoma armatum*, *E. sinensis*, *Macrophthalmus pacificus*, *Metopograpsus quadrident*, *Sesarma plicata*, *Parasesarma pictum*, *S. sinensis*, and *Alpheus bellulus*) obtained from previous research of our team (Wang et al., 2020; Shen et al., 2021; Wu et al., 2021; Wang et al., 2022; Zhu et al., 2022).

2.3 Identification and bioinformatics analysis of TLRs

The reference species was *L. vannamei*, which contains the most prominent *TLR* family genes in decapod crustaceans, but the names of *TLRs* were not unified. Therefore, the accurate number of *TLRs* in *L. vannamei* should be determined initially. The *TLRs* reported by Li et al. (2018) and Habib et al. (2021) in *L. vannamei* (Li et al., 2018; Habib et al., 2021), as well as the coding sequences (CDS) of other species (*Carcinus maenas*, *Daphnia pulex, D. melanogaster, E. sinensis, F. chinensis, M. rosenbergii, M. japonicas, P. monodon, P. trituberculatus, P. clarkii* and *S. serrata*) obtained from the NCBI database, were placed into the same FASTA file for sequence alignment using MEGA7.0 software (Kumar et al., 2016) (Table S1, Supplementary file 1). In this process, all nucleotide sequences of the CDS region were initially translated into the amino acid sequence, and then the sequence alignment was performed using Muscle v5 software (Edgar, 2004).

The phylogenetic tree of *L. vannamei* was constructed using the neighbor-joining (NJ) method in MEGA7.0 software by comparing the amino acid sequences. The Kimura 2-parameter model (K2P) was selected, and an optimal tree was obtained using the bootstrap method. The number of copies was set at 1000.

After confirming the accurate number of *TLR* genes in *L. vannamei*, the genomes of *E. sinensis*, *P. trituberculatus*, *P. platypus*, and *F. chinensis* were searched for using BLASTP. The number of *TLR* genes in the other four genomic species was initially determined, and the number of *TLR* genes from the transcriptome data was then determined. The obtained *TLR* sequences from the genome and transcriptome data were verified using MEGA7.0. The BLASTP program was used to search for homologous TLR protein sequences, and the results were compared with the nucleotide sequences. *TLR* genes with identical sequences were merged, and various *TLRs* were considered as single *TLR* genes. The integrity of *TLR* genes obtained from the transcriptome data was verified using cDNA libraries. If *TLR* sequences were incomplete, those larger than 300 bp were retained for subsequent analysis. The evolutionary relationships among different species of TLR proteins in decapods were analyzed using MEGA7.0 and FigTree v1.4.4 (Rambaut et al., 2018). Conserved protein functional domains were analyzed and annotated using the Simple Modular Structure Research Tool (SMART) program (https://smart.embl.de/smart/set_mode.cgi?NORMAL=1) (Letunic et al., 2021).

2.4 Selective pressure analysis of *TLRs* in decapod crustaceans

To investigate whether members of the *TLR* family in decapod crustaceans were affected by positive selection, selective pressure analysis was performed using PAML software (Yang, 2007). The CodeML program was used to estimate the synonymous replacement rates (*dS*) and non-synonymous replacement rates (*dN*). The ratio of ω (*dS* to *dN*) represents the change in selection pressure; $\omega > 1$, $\omega < 1$, and $\omega = 1$ denote positive, purified, and

neutral selection, respectively (Zhou et al., 2013). The site model (M8 and M8a site models) was used to detect the selection pressure on *TLR* genes in decapod crustaceans, and the branch-site model was evaluated for the main branches of shrimp and crabs (Brachyura B, *L. vannamei* and *F. chinensis*) (Yang and Nielsen, 2000). All the positive selected sites in both the site and branch-site models were identified by using Bayes Empirical Bayes (BEB) analysis with posterior probabilities greater than or equal to 0.80 (Yang, 2007). The significance of differences between the two nested models was conducted *via* likelihood ratio tests (LRTs) by calculating twice the log-likelihood (2InL) of the difference following a Chi-square distribution. The degrees of freedom were the difference in the number of free parameters between models (Guo et al., 2018).

2.5 WSSV challenges in *F. chinensis*

According to the method described by Sun et al. (2013), WSSV detection had been taken by One-step PCR before the infection experiment, and the sample was free of WSSV. Healthy *F. chinensis* were temporarily reared for a week after being returned to a temperature of 25°C and a salinity of 25%. During the temporary rearing process, oxygenation was continued to ensure an adequate oxygen supply. The water was changed daily, and the prawns were fed twice daily.

WSSV extracted from a WSSV-infected dying prawn was provided by Professor Fuhua Li at the Institute of Oceanology, Chinese Academy of Sciences. According to the method described by Sun et al. (2013), the DNA fragment of *VP28* gene encoding the extra-cellular part of the WSSV envelope protein VP28 was cloned into the pMD19T vector (TAKARA, Japan) and transfected into *E. coli* competent cells. The recombinant plasmids were extracted and quantified, and the copy number of WSSV was calculated. The plasmids were gradient diluted by ddH_2O to generate the standard curve of WSSV copy numbers ranging from 10^8 to 10^3. qRT-PCR was used to determine the concentration of virus particles and performed with primers qVP28F and qVP28R (Table 1) (Sun et al., 2013). The reaction system was as follows: 10 μL 2 × SuperReal PreMix Plus (TIANGEN, China), 2 μL diluted DNA template, 0.6 μL forward primer (10 μmol/L), 0.6 μL reverse primer (10 μmol/L), and 6.8 μL ddH_2O. The mixture was introduced into the ABI QuantStudio 3 quantitative PCR instrument (Applied Biosystems, USA), and the following procedure was procedures were conducted: pre-denaturation at 95°C °C for 15 min; denaturation at 95°C for 10 s, annealing at 55°Cfor 20 s, elongation at 72°C for 20 s, 45 cycles; dissolution curves were 95°C for 10 s, 65°C for 60 s, and 97°C for 1 s. The WSSV copy number per μL was calculated based on the standard curve. WSSV was diluted with PBS for further study. The experiment was divided into two groups: the WSSV group (experiment group) and the PBS group (control group), with 20 healthy *F. chinensis* in each group. The prawn in the experimental group was injected with 0.1 mL of WSSV virus (10^6 CFU/mL) in the third or fourth segments of their tails. The tails of prawns in the control group were injected with 0.1 mL of PBS solution. After 1 h and 24 h of injection, *F. chinensis* from the experimental and control groups were dissected separately, and hepatopancreas tissues were quickly frozen in liquid nitrogen.

2.6 Total RNA extraction and *TLRs* expression analysis

RNA was extracted from hepatopancreas tissues of *F. chinensis* using TRIzol reagent (TAKARA, Japan). cDNA libraries of different tissues were constructed according to the instructions of the PrimeScript™ Master Mix (TAKARA, Japan). Quantitative primers were designed using Primer 5.0 (Table 1). The expression levels of *TLR* genes in the WSSV and PBS groups at different infection time points were detected and analyzed using qRT-PCR.

TABLE 1 Primers used for quantitative real-time PCR.

Gene Name	Forward primer sequence (5′-3′)	Reverse primer sequence (5′-3′)
FcTLR1	TGGCAAACCTTACCATTCCCTA	CTCCTCACCATCACTGGCACA
FcTLR2	GTTTCTTCTATGGTGGCG	CAGTTTGGGCGTGTATTT
FcTLR3	CTCCGACGACCGAGATAA	TGTCACTGGCGTAGATGC
FcTLR4	GAACTTAGCCTTGAACCC	GACCCATCATACCTGTGC
FcTLR5	TCTGGTAGTGATGGCGATGC	TGTCCTTTAGCCCATCAACGT
FcTLR6	CGCACAAAGTGAACATACGCC	GAGACGCCTACCTCGGACA
FcTLR7	GCTGCGTGAGGAGCTTGTCGT	TGAGTCCGCTGGCATCGTTTG
FcTLR8	CTCCATTCCCTTCACATC	GTAGTCTCGGTCTCGTTGT
FcTLR9	TTCAAGTGCGACTGTAGCCT	TACTTGTCCGCTTCATCGTG
FcTLR10	CGAGCACCACAGAGCCAAGA	CACAGCCACCACGACGAACAT
ACTIN	GCGAGAAATCGTGCGTGAC	AGGGTGCGAGGGCAGTGAT
VP28	AAACCTCCGCATTCCTGTGA	TCCGCATCTTCTTCCTTCAT

The reaction system was as follows: 10 μL 2 × SuperReal PreMix Plus (TIANGEN, China), 2 μL cDNA template (50-fold dilution), 0.6 μL forward primer (10 μmol/L), 0.6 μL reverse primer (10 μmol/L), and 6.8 μL ddH_2O. The mixture was introduced into an ABI QuantStudio 3 quantitative PCR instrument (Applied Biosystems, USA), and the following procedures were conducted: pre-denaturation at 95°C for 15 min; denaturation at 95°C for 10 s, annealing at 55°C for 20 s, elongation at 72°C for 20 s, 45 cycles; dissolution curves were 95°C for 10 s, 65°C for 60 s, and 97°C for 1 s. The $2^{-\Delta CT}$ method (Visser et al., 2011) was used to calculate the relative expression level of the target gene relative to the internal reference *ACTIN*. The calculation method is as follows: $\Delta CT=CT^T-CT^G$; relative transcript level = $2^{-\Delta CT}$(CT, cycle threshold; CT^T is CT value of target gene; CT^G is CT value of internal reference gene *ACTIN*).

Significance was conducted using Independent-Samples T Test by SPSS Statistics 23 (Field, 2013). Different experiment groups (1 h PBS vs. 1 h WSSV group, or 1 h WSSV group vs. 24 h WSSV group) were set as Grouping Variable, whereas the relative expression level of *FcTLRs* was set as Test Variable. * and ** indicated statistically significant differences at $P<0.05$ and $P<0.01$, respectively. Histogram drawing was performed using GraphPad Prism 7.0 (Swift, 1997).

3 Result

3.1 Identification of *TLR* genes

Nine *TLR* genes reported by Li et al. (2018) and 11 genes reported by Habib et al. (2021) were aligned to construct phylogenetic trees for *L. vannamei* (Li et al., 2018; Habib et al., 2021). A total of eight *TLRs* genes were conserved between the two study groups (*PTL-2* and *Lv-Toll2*, *PTL-1* and *Lv-Toll1*, *TLR-13x* and *Lv-Toll9*, *TLR-Tollo4* and *Lv-Toll5*, *TLR-6* and *Lv-Toll6*, *TLR-Tollo2* and *Lv-Toll4*, *TLr-Tollo3* and *Lv-Toll8*, *TLR* and *Lv-Toll3*) and clustered in the near branch. The remaining *Lv-Toll7*, *TLR-13*, *TLR-3*, and *TLR-4* were grouped dispersedly in separate branches. Therefore, 12 *TLR* genes were identified in *L. vannamei* (Figure 1, Table S2). In the present study, *Toll1–9*, reported by Li et al. (2018), were named *LvTLR1–9*, whereas *TLR-3*, *TLR-4*, and *TLR-13* in the Habib et al. (2021) were named as *LvTLR10*, *LvTLR11*, and *LvTLR12*, respectively (Figure 1, Table S2). Ten *TLR* genes were identified using a BLASTP search with genomic and transcriptome data in both *F. chinensis* (*FcTLR1–10*) and *P. trituberculatus* (*PtTLR1–9, PtTLR11*), seven complete *TLRs* genes were identified in *E. sinensis* (*EsTLR1–5 and EsTLR7–8*), and seven *TLRs* genes were identified in *P. gigas* (*PgTLR1–6 and PgTLR9*). There were relatively

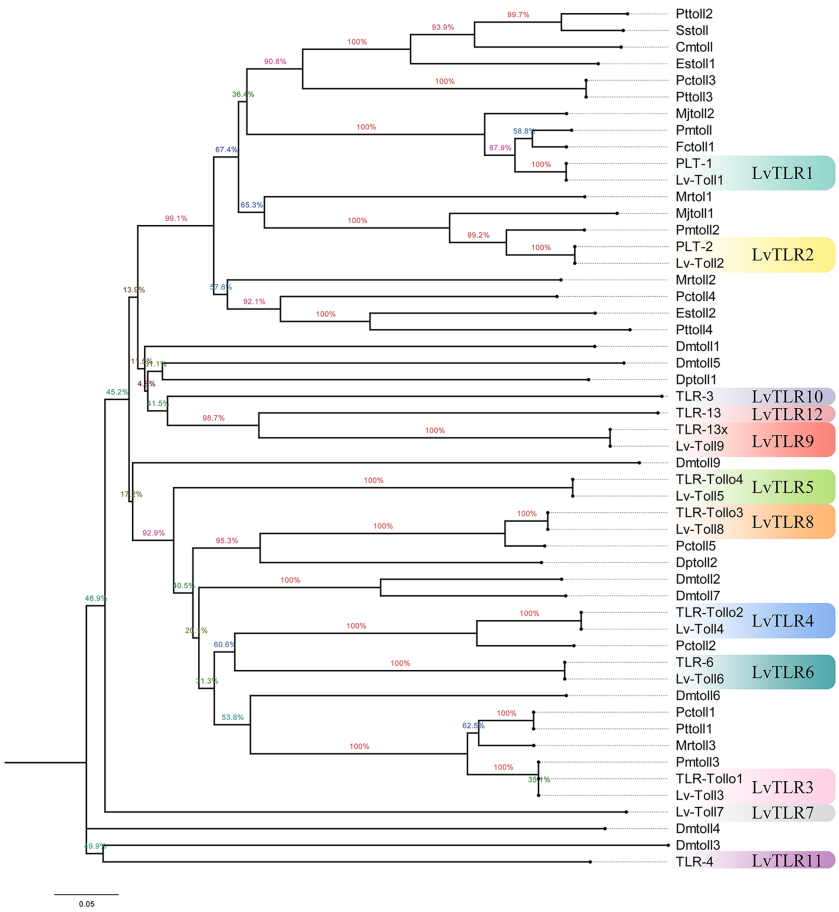

FIGURE 1
Construction of a unified naming system of *TLR* genes in decapods according to the previous two naming systems in *L.vannamei*.

few complete *TLR* genes from the other transcriptome data, and most of the sequences were incomplete (Table 2). Eight *TLR* gene sequences were found in *P. clarkii*, and only four had complete CDS (*PcTLR1–3* and *PcTLR6*). Only the intermediate sequences of *PcTLR4*, *PcTLR5* and the 3'UTR of *PcTLR7* and *PcTLR8* were obtained. Seven *TLR* gene sequences were found in *C. armatum*, and *CaTLR2*, *CaTLR4*, *CaTLR7*, and *CaTLR8* had complete CDS sequences, *CaTLR1* and *CaTLR3* had incomplete 5'UTR, and *CaTLR6* had only partial intermediate sequences. Transcripts longer than 300 bp were retained for subsequent analysis. Phylogenetic analysis displayed that different TLR proteins were clustered in similar clusters, which were divided into 10 categories, and each type of TLR protein was concentrated in the same category. Prawns were further aggregated, and the internal genetic distances were relatively close (Figure 2).

3.2 Prediction of the functional domain of the TLR proteins

SMART was used for protein domain prediction to determine whether the nucleotide sequence obtained from BLASTP represented *TLR* genes. Most typical TLRs contain a signal peptide, LRR domains, a transmembrane domain, and an intracellular toll-interleukin receptor (TIR) domain; similar characteristics were found in *L. vannamei* and *F. chinensis*. The number of LRR domain repeats in *L. vannamei* (Figure 3), *F. chinensis* (Figure 4), and *E. sinensis* (Figure 5) ranged from 5 (*LvTLR12* to 25 (*LvTLR8*), 4 (*FcTLR7*) to 25 (*FcTLR8*), and 9 (*EsTLR1*) to 25 (*EsTLR3*), respectively.

3.3 Selective pressure analysis of *TLRs* in decapod crustaceans

M8 and M8a of the site model are used to represent the selection pressure received by each site. In the present study, the positive selection model M8 of the *TLR1*, *TLR2*, *TLR7*, and *TLR9* genes was better than the neutral model M8a, and the ω values of the four genes were 5.16, 8.07, 1.53, and 5.14 (ω>1), indicating a strong positive selection. There were two positively selected sites in *TLR1* (325 0.812, 505 0.838), one positively selected site in *TLR2* (599 0.816), 11 positively selected sites in *TLR7* (172 0.932, 175 0.899, 186 0.838, 359 0.922, 361 0.803, 388 0.894, 391 0.870, 856 0.839, 959 0.923, 965 0.848, and 975 0.918), and four positively selected sites in *TLR9* (239 0.803, 616 0.813, 699 0.957, and 904 0.821) (Table 3).

We then used the branch-site model to analyze the branches of Brachyura (B), *L. vannamei* (*Lv*), and *F. chinensis* (*Fc*) in the *TLR* gene dataset of decapod crustaceans. Four (*TLR1*, *TLR6*, *TLR7*, and *TLR9*) of nine *TLR* family genes were also found to be under positive selection in decapod crustaceans, where the LRTs of the branch-site model were statistically significant (Table 4). *TLR1* and *TLR9* detected positive selection signals in Brachyura (B), which had three (153, 218, and 25) and seven (368, 378, 380, 390, 412, 415, and 859) positively selected sites, respectively. *TLR9* also detected positive selection signals in *L. vannamei* (*Lv*) with two (605 and 760) positively selected sites. *TLR7* did not detect positive selection signals in Brachyura (B), *F. chinensis* (*Fc*), and *L. vannamei* (*Lv*), but detected positive selection signals in *F. chinensis* (*Fc*) with seven (368, 378, 380, 381, 383, 412, and 859) positively selected sites. In addition, *TLR6* detected a positive selection signal in *L. vannamei* (*Lv*) with one (545) positively selected site (Table 4).

TABLE 2 Identification of *TLR* genes in decapod crustaceans*.

	TLR1	*TLR2*	*TLR3*	*TLR4*	*TLR5*	*TLR6*	*TLR7*	*TLR8*	*TLR9*	*TLR10*	*TLR11*	*TLR12*
L. Vannamei	●	●	●	●	●	●	●	●	●	●	●	●
F. chinensis	●	●	●	●	●	●	●	●	●	●		
E. sinensis	●	●	●	●	●			●	●			
P. trituberculatus	●	●	●	●	●	●	●	●	●		●	
P. gigas	●	●	●	●	●	●			●			
P. clarkii [a]	●	●	●	▲	▲	●	3'	3'				
C. Armatum [a]	5'	●	5'	●		▲	●	●				
E. sinensis [a]		▲	3'		▲	▲			●			
M. pacificus [a]		▲				▲						
M. quadridentatus [a]		▲		3'					●			
S. plicata [a]									5'			
P. Pictum [a]			▲						5'			
S. sinensis [a]		▲										
A. bellulus [a]							▲					

* ● represents complete coding sequence; ▲ represents the middle part of the sequence; 5' and 3' represent the 5' and 3' end of CDS region, respectively. [a] indicates the data was obtained from transcriptome.

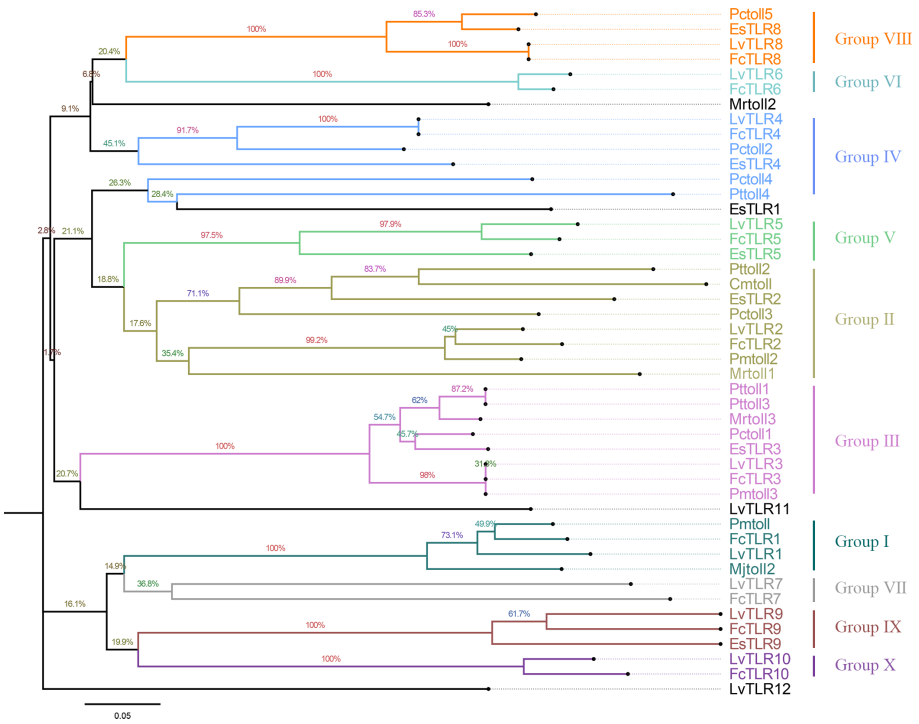

FIGURE 2
Phylogenic analysis of TLR protein sequences in decapods (neighbor-joining tree).

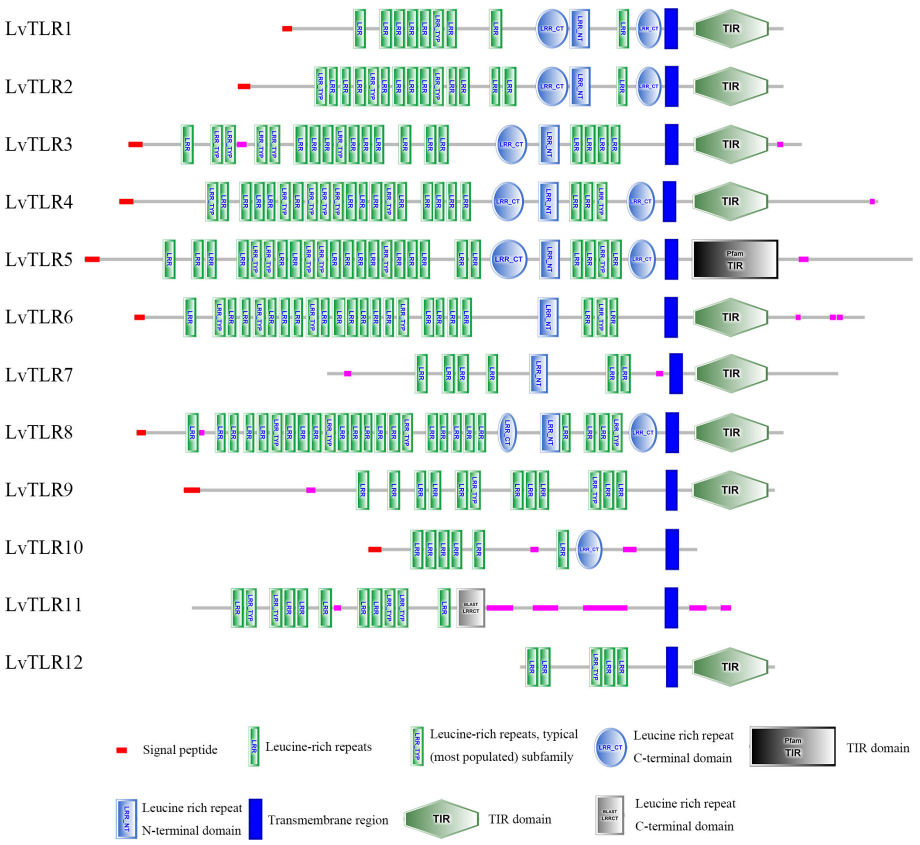

FIGURE 3
Protein domain analysis of the 12 LvTLR proteins in *L. vannamei*.

10.3389/fevo.2023.1175220

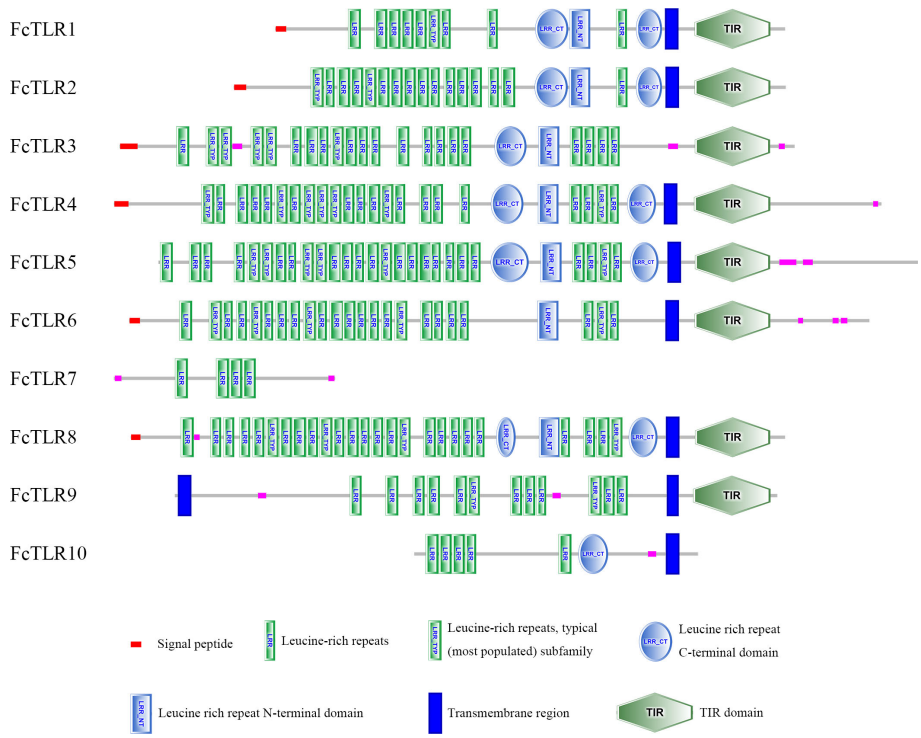

FIGURE 4
Protein domain analysis of the 10 FcTLR proteins in *F. chinensis*.

3.4 Expression analysis of *FcTLRs* in *F. chinensis* under WSSV challenge

The expression levels of *FcTLR1–10* in *F. chinensis* were detected by 1-h short-term infection and 24-h long-term WSSV infection in the experimental group, and PBS solution was injected in the PBS group as a control. The expression levels of *FcTLR7* and *FcTLR9* significantly increased in the 1-h short-term WSSV infection, while their expression levels decreased following 24-h WSSV infection. The expression level of *FcTLR1* had no significant difference in the 1-h WSSV infection, compared with 1-h PBS, but *FcTLR1* represented a significant response in the 24-h infection

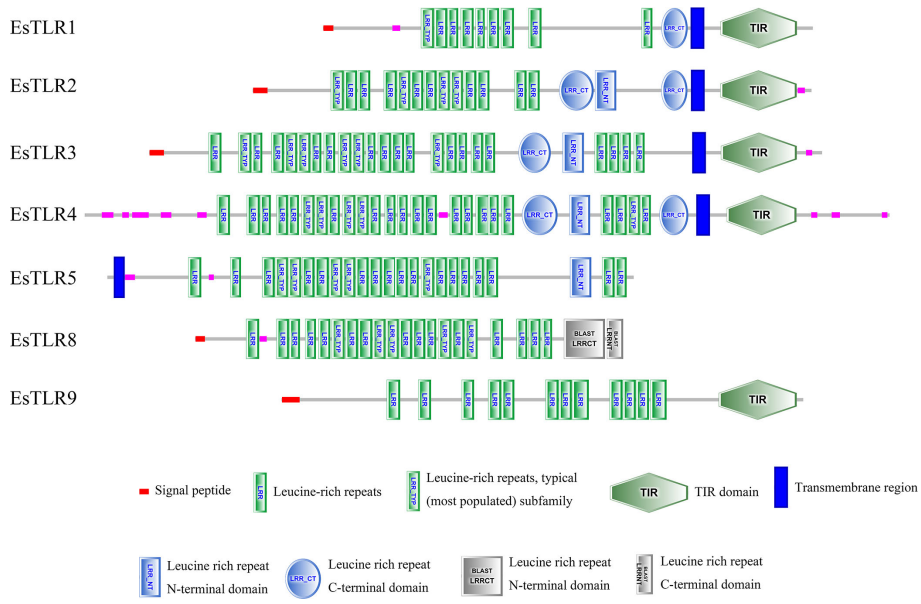

FIGURE 5
Protein domain analysis of the 7 EsTLR proteins in *E. sinensis*.

TABLE 3 Selective pressure analyses (M8 and M8a site models) of nine *TLR* genes in decapod crustaceans[a].

Gene	ln_M8a	ln_M8	2lnL	*P* value	ω value	Positive selected sites
TLR1	−12745.23326	−12741.82251	6.821496	0.009006	5.15682	325 0.812 505 0.838
TLR 2	−15435.04939	−15430.52841	9.041974	0.002638	8.07432	599 0.816
TLR 3	−12946.60537	−12946.60537	0.000	1.000	1.000000	
TLR 4	−15656.20063	−15656.20063	0.000	1.000	1.000000	
TLR 5	−14041.98676	−14041.98676	0.000	1.000	1.000000	
TLR 6	−16747.38272	−16747.38272	−4E−06	1.000	1.000000	
TLR 7	−10645.07466	−10644.57474	0.99984	0.317349	1.53089	172 0.932 359 0.922 391 0.870 965 0.848 175 0.899 361 0.803 856 0.839 186 0.838 959 0.923 975 0.918 388 0.894
TLR 8	−12977.70037	−12977.70037	0.000	1.000	1.000000	
TLR 9	−15635.05141	−15628.85063	12.40155	0.000429	5.14341	239 0.803 616 0.813 699 0.957 904 0.821

[a]**In M8:** Assume all sites 0 < ω <1 or ω>1, with beta distribution; **InM8a,** Assume all sites 0 < ω <1 or ω=1, with beta distribution; **2InL,** twice the logarithmic likelihood. **ω value:** The ratio (ω = dN/dS) of nonsynonymous to synonymous substitutions rate was estimated for selective constraint, where ω > 1, = 1, and <1 respectively indicate positive, neutral, and purifying selection.

TABLE 4 Selective pressure analyses (branch-site model) of nine *TLR* genes in decapod crustaceans[a].

Gene	Model	lnL	2lnL	*P* level	Parameters	Positive selected sites
TLR1	**B**					
	ma	−12784.846			ω0 = 0.093 ω1 = 1.0 ω2 = 2.715	153 0.950* 218 0.954* 25 0.953*
	ma0	−12787.896	6.100142	0.013517	ω0 = 0.09 ω1 = 1.0 ω2 = 1.0	
	Fc					
	ma	−12798.47			ω0 = 0.098 ω1 = 1.0 ω2 = 1.0	
	ma0	−12798.47	0	1	ω0 = 0.098 ω1 = 1.0 ω2 = 1.0	
	Lv					
	ma	−12797.514			ω0 = 0.096 ω1 = 1.0 ω2 = 1.0	
	ma0	−12797.514	0	1	ω0 = 0.096 ω1 = 1.0 ω2 = 1.0	
TLR2	**B**					
	ma	−15485.769			ω0 = 0.11 ω1 = 1.0 ω2 = 1.0	
	ma0	−15485.769	0	1	ω0 = 0.11 ω1 = 1.0 ω2 = 1.0	
	Fc					
	ma	−15480.564			ω0 = 0.111 ω1 = 1.0 ω2 = 8.791	
	ma0	−15483.362	5.595322	0.018009	ω0 = 0.11 ω1 = 1.0 ω2 = 1.0	
	Lv					
	ma	−15486.948			ω0 = 0.113 ω1 = 1.0 ω2 = 1.0	
	ma0	−15486.948	0	1	ω0 = 0.113 ω1 = 1.0 ω2 = 1.0	
TLR3	**B**					
	ma	−13010.772			ω0 = 0.037 ω1 = 1.0 ω2 = 998.984	

(Continued)

TABLE 4 Continued

Gene	Model	lnL	2lnL	*P* level	Parameters	Positive selected sites
	ma0	−13014.628	7.712554	0.005484	ω0 = 0.036 ω1 = 1.0 ω2 = 1.0	
	Fc					
	ma	−13029.506			ω0 = 0.039 ω1 = 1.0 ω2 = 1.0	
	ma0	−13029.506	0	1	ω0 = 0.039 ω1 = 1.0 ω2 = 1.0	
	Lv					
	ma	−13029.506			ω0 = 0.039 ω1 = 1.0 ω2 = 1.0	
	ma0	−13029.506	0	1	ω0 = 0.039 ω1 = 1.0 ω2 = 1.0	
TLR4	**B**					
	ma	−15664.312			ω0 = 0.03 ω1 = 1.0 ω2 = 65.709	
	ma0	−15666.895	5.167332	0.023016	ω0 = 0.028 ω1 = 1.0 ω2 = 1.0	
	Fc					
	ma	−15689.899			ω0 = 0.03 ω1 = 1.0 ω2 = 1.0	
	ma0	−15689.899	0	1	ω0 = 0.03 ω1 = 1.0 ω2 = 1.0	
	Lv					
	ma	−15689.401			ω0 = 0.03 ω1 = 1.0 ω2 = 1.0	
	ma0	−15689.401	0	1	ω0 = 0.03 ω1 = 1.0 ω2 = 1.0	
TLR5	**B**					
	ma	−14049.918			ω0 = 0.036 ω1 = 1.0 ω2 = 999.0	
	ma0	−14065.634	31.43218	0	ω0 = 0.031 ω1 = 1.0 ω2 = 1.0	
	Fc					
	ma	−14090.91			ω0 = 0.037 ω1 = 1.0 ω2 = 1.0	
	ma0	−14090.91	0	1	ω0 = 0.037 ω1 = 1.0 ω2 = 1.0	
	Lv					
	ma	−14091.749			ω0 = 0.038 ω1 = 1.0 ω2 = 1.0	
	ma0	−14091.561	−0.37605	1	ω0 = 0.037 ω1 = 1.0 ω2 = 1.0	
TLR6	**B**					
	ma	−16823.765			ω0 = 0.029 ω1 = 1.0 ω2 = 44.54	
	ma0	−16794.793	−57.9425	1	ω0 = 0.026 ω1 = 1.0 ω2 = 1.0	
	Fc					
	ma	−16823.765			ω0 = 0.029 ω1 = 1.0 ω2 = 1.0	
	ma0	−16823.765	0	1	ω0 = 0.029 ω1 = 1.0 ω2 = 1.0	
	Lv					
	ma	−16821.402			ω0 = 0.029 ω1 = 1.0 ω2 = 13.521	545 0.957*
	ma0	−16823.765	4.726142	0.029707	ω0 = 0.029 ω1 = 1.0 ω2 = 1.0	
TLR7	**B**					
	ma	−10643.226			ω0 = 0.049 ω1 = 1.0 ω2 = 999.0	

(Continued)

TABLE 4 Continued

Gene	Model	lnL	2lnL	*P* level	Parameters	Positive selected sites
	ma0	−10646.594	6.73536	0.009452	ω0 = 0.042 ω1 = 1.0 ω2 = 1.0	
	Fc					
	ma	−10635			ω0 = 0.042 ω1 = 1.0 ω2 = 19.648	368 0.994** 378 0.996** 380 0.998** 381 0.983* 383 0.988* 412 0.991** 859 0.992**
	ma0	−10635.599	1.381402	0.239862	ω0 = 0.036 ω1 = 1.0 ω2 = 1.0	
	Lv					
	ma	−10645.018			ω0 = 0.047 ω1 = 1.0 ω2 = 6.474	
	ma0	−10644.915	−0.20504	1	ω0 = 0.049 ω1 = 1.0 ω2 = 1.0	
TLR8	**B**					
	ma	−13082.354			ω0 = 0.023 ω1 = 1.0 ω2 = 14.801	
	ma0	−13082.353	−0.00147	1	ω0 = 0.023 ω1 = 1.0 ω2 = 1.0	
	Fc					
	ma	−13082.231			ω0 = 0.023 ω1 = 1.0 ω2 = 1.0	
	ma0	−13082.231	0	1	ω0 = 0.023 ω1 = 1.0 ω2 = 1.0	
	Lv					
	ma	−13082.353			ω0 = 0.023 ω1 = 1.0 ω2 = 1.0	
	ma0	−13082.353	0	1	ω0 = 0.023 ω1 = 1.0 ω2 = 1.0	
TLR9	**B**					
	ma	−15701.442			ω0 = 0.075 ω1 = 1.0 ω2 = 999.0	368 0.994** 378 0.996** 380 0.998** 390 0.990** 412 0.991** 415 0.994** 859 0.992**
	ma0	−15726.22	49.55767	0	ω0 = 0.07 ω1 = 1.0 ω2 = 1.0	
	Fc					
	ma	−15735.486			ω0 = 0.07 ω1 = 1.0 ω2 = 1.0	
	ma0	−15735.486	0	1	ω0 = 0.07 ω1 = 1.0 ω2 = 1.0	
	Lv					
	ma	−15726			ω0 = 0.065 ω1 = 1.0 ω2 = 1.0	605 0.991** 760 0.965*
	ma0	−15725.985	0	1	ω0 = 0.065 ω1 = 1.0 ω2 = 1.0	

[a]**lnL,** logarithmic likelihood; **2lnL,** twice the logarithmic likelihood; **B**, Brachyura; **Fc**, F. chinensis; **Lv**, L. vannamei; The alternative (**ma**, positive selection: 0<ω0<1, ω1 = 1, ω2≥1) and the null model (**ma0**, neutral evolution with ω2 = 1 fixed) in the branch-site test were used to detect selective pressure on each branch.

group. The expression levels of *FcTLR2* and *FcTLR8* decreased in the 1-h WSSV infection, but their expression levels had no significant difference in the 24-h WSSV infection. Besides, the expression levels of *FcTLR3*, *FcTLR4*, *FcTLR5*, *FcTLR6*, and *FcTLR10* have no significant difference following WSSV infection (Figure 6).

4 Discussion

TLRs are essential membrane receptors in the TLR signaling pathway and play an important role in innate immunity against pathogens. To date, *TLR* genes have been extensively acknowledged in vertebrates, such as humans, mice, common carp, and spotted sea bass, but are relatively rare in decapod crustaceans (Roach et al., 2005; Gong et al., 2017; Fan et al., 2019; Habib et al., 2021). Decapod crustaceans exhibit a broad distribution across diverse habitats, and their growth characteristics are influenced by a range of ecological factors, including temperature. The *TLR* gene is a crucial component of innate immunity in invertebrate, and its reaction to environmental stimuli may vary among distinct crustacean species. This study compared *TLR* gene sequences of decapod crustaceans from NCBI and our laboratory, and a unified naming system was developed. A total of nine *TLR* genes from Li et al. (2018) and 11

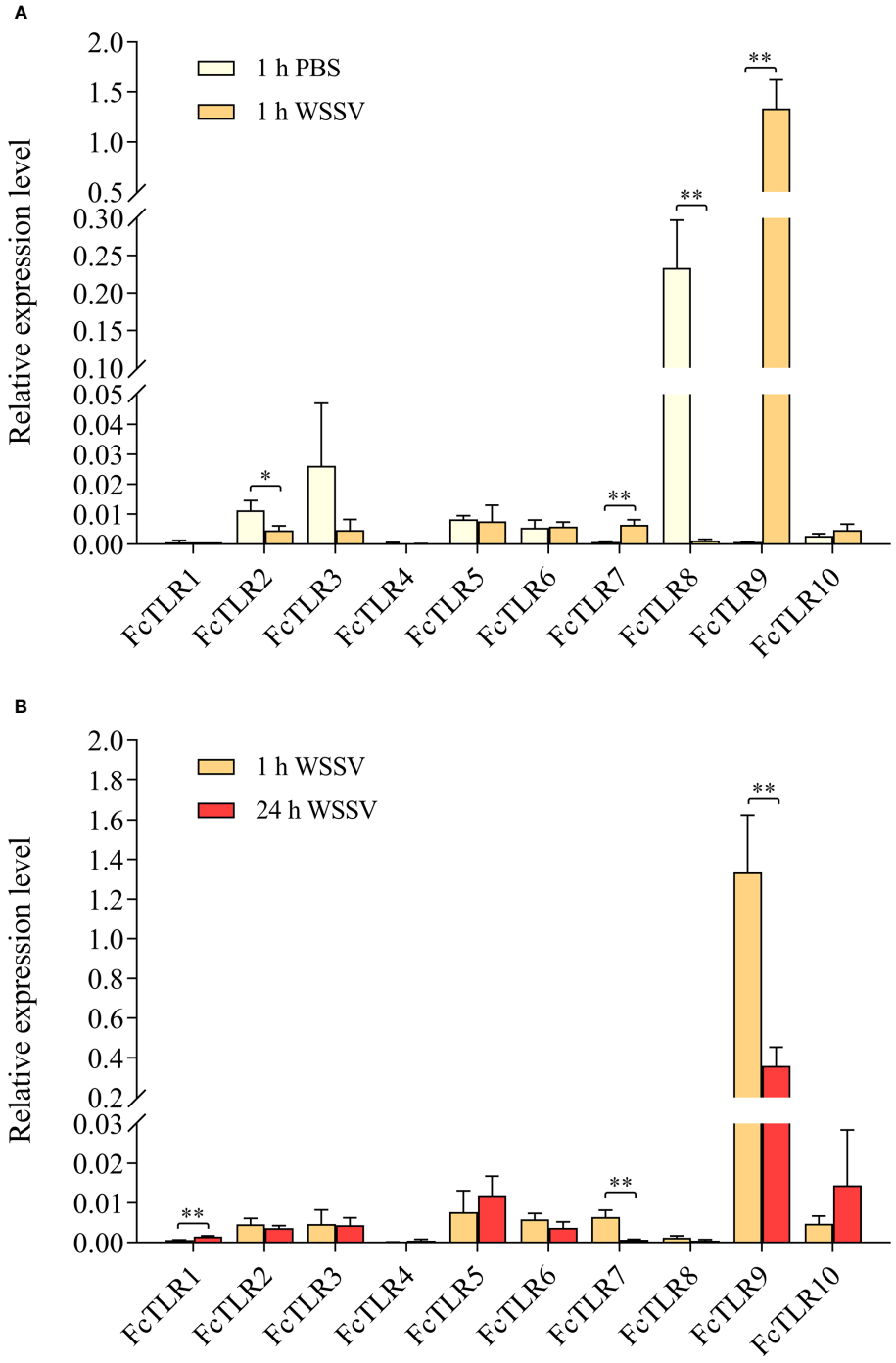

FIGURE 6
The relative expression level of 10 *FcTLRs* in *F. chinensis* infected with WSSV. **(A)** the relative expression level of *FcTLRs* between the 1 h PBS group and 1 h WSSV group at the 1-h time point; **(B)** the relative expression level of *FcTLRs* in the WSSV group between the 1-h time point and the 24-h time point. The data are the mean± SD of three independent biological replicates, n=3 hepatopancreas. * and ** indicate statistical significance at $P<0.05$ and $P<0.01$ by Student's *t*-test, respectively.

TLR genes from Habib et al. (2021) in *L. vannamei* were renamed as 12 *TLR* genes (Li et al., 2018; Habib et al., 2021). In the present study, two relatively complete *TLRs* gene families in *F. chinensis* (10 *TLRs*) and *E. sinensis* (7 *TLRs*) were annotated using the BLASTP program to BLAST other available RNA and genome databases in decapod crustaceans. Because of some limitations in the genome and transcriptome data quality, some *TLR* genes obtained contained only the 5'UTR, 3'UTR, or intermediate cDNA fragments. Complete *TLR9* was annotated in *E. sinensis* and *M. quadridentatus* in the RNA database of our lab, and partial sequences of the *TLR* genes were obtained for the remaining species (*P. clarkia*, *C. armatum*, *M. pacificus*, *M. quadridentatus*, *S. plicata*, *P. pictum*, *S. sinensis*, *A. bellulus*) in our databases. This may be related to the tissue-specific expression of the *Toll* gene and

the size restriction of the transcriptome. In the future, high-quality publications of shrimp and crab genomes will allow for the discovery of *TLR* genes. According to multiple sequence alignment and NJ phylogenetic tree construction, different species of TLR proteins were clustered in one group. *F. chinensis* and *L. vannamei* had the highest TLR homology and were clustered in the near branch. They have higher homology with shrimp families and a greater relationship with carbs, such as *E. sinensis* (Figure 2). This suggests that more closely related species have a higher sequence homology.

Analysis of the gene-conserved protein domain revealed domains typical of TLRs in mammals, bony fish, and crustaceans, including signaling peptides, extracellular LRR domains, transmembrane domains, and intracellular toll-interleukin receptors (TIR). LRRs are associated with pathogen recognition, and the intracellular TIR domain acts as a connector to initiate downstream signaling. Furthermore, TLR domain analysis revealed the existence of multiple extracellular LRR domains in PtToll1, ranging from 5 to 25, similar to the 13–25 LRR domains reported in previous studies (Zhang et al., 2018). In the present study, 4–25 LRR domains of FcTLRs were also found in *F. chinensis*, indicating that the TLRs were highly conserved and that various TLRs might be used to respond to different pathogens. This result was similar to that of protein domain analysis of TLRs in *L. vannamei*. TLRs, an important pattern recognition protein, are essential for innate immunity. The analysis of protein domains revealed that they had different repeats of LRR domains, indicating that TLRs may have changed differently in response to various pathogen invasion environments during the long evolutionary process.

The adaptation of gene function is based on the long-term adaptive evolution of the genome sequence and the rapid adaptation of changes in gene expression to environmental changes. There are few systematic descriptions of the interspecific genomic changes in TLR pathway genes in decapod crustaceans, especially in specific variation sites, functional analysis at the domain level, and the study of gene evolution rate. The phylogenetic relationship tree of the *TLR* gene family can help us to understand the functional differentiation of family genes. This provides substantial evidence for determining *TLR* gene function. In general, the ω values of most genes are equal to one, that is, neutral selection. When $\omega > 1$ and the posterior probabilities at the positive selection site is greater than 0.8, the site is considered under positive selection pressure (Zhou et al., 2013). Positive selection signals were detected in the *TLR1* (5.16), *TLR2* (8.07), *TLR7* (1.53), and *TLR9* (5.14) genes of decapod crustaceans by site model analysis. Moreover, positive selection signals were detected in *TLR1* ($P<0.05$, $\omega2 = 2.72$) and *TLR9* ($P<0.01$, $\omega2 = 999.00$) in Brachyura (B), *TLR6* ($P<0.05$, $\omega2 = 13.52$) in *L. vannamei* (*Lv*) using a branch-site model. By combining the site and branch-site model analysis results, *TLR1* and *TLR9* were subjected to positive selection during the evolutionary process in decapod crustaceans.

RNAi of *Toll4* in *L. vannamei* showed that prawns became more sensitive to WSSV infection as the virus load increased (Li et al., 2018). *TLRs* in *S. serrata* (*SsToll*), *P. clarkia* (*PcToll3*, *PcToll5*, and *PcToll6*), *S. paramamosain* (*SpToll2*) exhibited positive responses to the WSSV challenge (Vidya et al., 2014; Lan et al., 2016; Chen et al., 2018; Huang et al., 2018). qRT-PCR was used to detect *TLR* genes in the hepatopancreas of *F. chinensis* infected with WSSV, and the results indicated that *FcTLR1*, *FcTLR7*, and *FcTLR9* exhibited positive responses, suggesting that they may play an essential role in WSSV stress adaptation. This study also provides a reference for other health aquaculture systems. Positive selection signals were detected for *TLR1*, *TLR7*, and *TLR9*, suggesting that different *TLR* genes in decapod crustaceans may respond differently to various pathogens.

This study identified 10 *FcTLR* family genes and analyzed their functional domains in *F. chinensis*. The expression level of *FcTLR* family genes under WSSV challenge was detected in *F. chinensis*, and it was examined whether the *TLR* genes in decapod crustaceans were driven by positive selection to explore the gene adaptation and functional differentiation of *TLRs*. Discussing these issues provides new insights into the immune defense mechanism and cultivation of healthy decapod crustaceans to prevent environmental damage, such as pathogens and temperature.

5 Conclusion

This study comprehensively studied the molecular characterization, adaptive evolution, and expression analysis of *TLR* genes in *F. chinensis*. Ten *TLR* genes in *F. chinensis* and seven *TLR* genes in *E. sinensis* were identified using genome-wide analysis, and their protein domains were relatively conserved. Most TLR proteins contain a typical leucine repeat domain, a transmembrane region, an interleukin receptor domain, and other structures, but the number of LRR in different TLRs varies from 4 (*FcTLR7*) to 25 (*FcTLR8*), which might be related to their response to various pathogens. In the selection pressure analysis, M8 and M8a of the site model and branch-site models were used to determine the selection pressure of the currently available *TLR* genes in decapod crustaceans. Positive selection signals were detected in some genes, such as *TLR1* and *TLR9*, indicating that these genes were subjected to positive selection during the evolutionary process. Finally, the expression of the *FcTLR* genes after WSSV infection was detected in *F. chinensis*. The stress time was detected at 1 h and 24 h. *FcTLR7* and *FcTLR9* revealed strong positive responses at the 1-h time point, whereas *FcTLR1* revealed strong positive responses at the 24-h time point. These results indicate that *FcTLR1*, *FcTLR7*, and *FcTLR9* could be essential in response to WSSV infection in *F. chinensis*, consistent with protein domain and selective pressure analyses.

Data availability statement

The original contributions presented in the study are included in the article/Supplementary Material. Further inquiries can be directed to the corresponding author.

Author contributions

LC and ZW conceived and designed the experiments. LC analyzed the data and wrote the manuscript. DT performed the

main experimental work. YH was involved in the drawing of phylogenetic trees and protein domain analysis. XW and YL participated in the feeding and anatomy of samples. All authors participated in editing the manuscript and have approved the final manuscript.

Funding

This research was funded by the Jiangsu Provincial Double-Innovation Doctor Program, Jiangsu Province, China (JSSCBS20211141).

Acknowledgments

We are grateful to Professor Fuhua Li of the Institute of Oceanology, Chinese Academy of Sciences for the supply of WSSV. We thank Home for Researchers editorial team (www.home-for-researchers.com) for language editing service.

Conflict of interest

The authors declare that the research was conducted in the absence of any commercial or financial relationships that could be construed as a potential conflict of interest.

Publisher's note

Supplementary material

The Supplementary Material for this article can be found online at: https://www.frontiersin.org/articles/10.3389/fevo.2023.1175220/full#supplementary-material

References

Arts, J. A. J., Cornelissen, F. H. J., Cijsouw, T., Hermsen, T., Savelkoul, H. F. J., and Stet, R. J. M. (2007). Molecular cloning and expression of a toll receptor in the giant tiger shrimp, *Penaeus monodon*. *Fish Shellfish Immunol.* 233, 504–513. doi: 10.1016/j.fsi.2006.08.018

Assavalapsakul, W., and Panyim, S. (2012). Molecular cloning and tissue distribution of the toll receptor in the black tiger shrimp, *Penaeus monodon*. *Genet. Mol. Res.* 11, 484–493. doi: 10.4238/2012.March.6.1

Barton, G. M., and Kagan, J. C. (2009). A cell biological view of toll-like receptor function: regulation through compartmentalization. *Nat. Rev. Immunol.* 9, 535–542. doi: 10.1038/nri2587

Bondad-Reantaso, M. G., Subasinghe, R. P., Arthur, J. R., Ogawa, K., Chinabut, S., Adlard, R., et al. (2005). Disease and health management in Asian aquaculture. *Vet. Parasitol.* 132, 249–272. doi: 10.1016/j.vetpar.2005.07.005

Chen, Y., Aweya, J. J., Sun, W., Wei, X., Gong, Y., Ma, H., et al. (2018). *SpToll1* and *SpToll2* modulate the expression of antimicrobial peptides in *Scylla paramamosain*. *Dev. Comp. Immunol.* 87, 124–136. doi: 10.1016/j.dci.2018.06.008

Chen, H., Liang, Y., Han, Y., Liu, T., and Chen, S. (2020). Genome-wide analysis of toll-like receptors in zebrafish and the effect of rearing temperature on the receptors in response to stimulated pathogen infection. *J. Fish Dis.* 44, 337–349. doi: 10.1111/jfd.13287

Chiang, C., and Beachy, P. A. (1994). Expression of a novel *Toll-like* gene spans the parasegment boundary and contributes to hedgehog function in the adult eye of *Drosophila*. *Mech. Dev.* 47, 225–239. doi: 10.1016/0925-4773(94)90041-8

Edgar, R. C. (2004). MUSCLE: multiple sequence alignment with high accuracy and high throughput. *Nucleic Acids Res.* 32, 1792–1797. doi: 10.1093/nar/gkh340

Fan, H., Wang, L., Wen, H., Wang, K., Qi, X., Li, J., et al. (2019). Genome-wide identification and characterization of *toll-like receptor* genes in spotted sea bass (*Lateolabrax maculatus*) and their involvement in the host immune response to *Vibrio harveyi* infection. *Fish Shellfish Immunol.* 92, 782–791. doi: 10.1016/j.fsi.2019.07.010

Feng, J., Zhao, L., Jin, M., Li, T., Wu, L., Chen, Y., et al. (2016). Toll receptor response to white spot syndrome virus challenge in giant freshwater prawns (*Macrobrachium rosenbergii*). *Fish Shellfish Immunol.* 57, 148–159. doi: 10.1016/j.fsi.2016.08.017

Field, A. (2013). *Discovering statistics using IBM SPSS statistics* (Los Angeles: SAGE).

Gao, N., Lu, X., Yan, Y., Kong, J., Meng, X., Li, X., et al. (2023). Cloning and expression of *FcBMP-7* gene in Chinese shrimp *Fenneropenaeus chinensis*. *Fish Sci.* 42, 347–356. doi: 10.16378/j.cnki.1003-1111.21023

Gong, Y., Feng, S., Li, S., Zhang, Y., Zhao, Z., Hu, M., et al. (2017). Genome-wide characterization of toll-like receptor gene family in common carp (*Cyprinus carpio*) and their involvement in host immune response to *Aeromonas hydrophila* infection. *Comp. Biochem. Physiol. Part D Genomics Proteomics* 24, 89–98. doi: 10.1016/j.cbd.2017.08.003

Guo, H., Yang, H., Tao, Y., Tang, D., Wu, Q., Wang, Z., et al. (2018). Mitochondrial *OXPHOS* genes provides insights into genetics basis of hypoxia adaptation in anchialine cave shrimps. *Genes Genom.* 40, 1169–1180. doi: 10.1007/s13258-018-0674-4

Habib, Y. J., Wan, H., Sun, Y., Shi, J., Yao, C., Lin, J., et al. (2021). Genome-wide identification of toll-like receptors in pacific white shrimp (*Litopenaeus vannamei*) and expression analysis in response to *Vibrio parahaemolyticus* invasion. *Aquaculture* 532, 735996. doi: 10.1016/j.aquaculture.2020.735996

Habib, Y. J., and Zhang, Z. (2020). The involvement of crustaceans toll-like receptors in pathogen recognition. *Fish Shellfish Immunol.* 102, 169–172. doi: 10.1016/j.fsi.2020.04.035

Hoshino, K., Takeuchi, O., Kawai, T., Sanjo, H., Ogawa, T., Takeda, Y., et al. (1999). Cutting edge: toll-like receptor 4 (TLR4)-deficient mice are hyporesponsive to lipopolysaccharide: evidence for TLR4 as the *Lps* gene product. *J. Immunol.* 162, 3749–3752. doi: 10.4049/jimmunol.162.7.3749

Huang, Y., Chen, Y., Hui, K., and Ren, Q. (2018). Cloning and characterization of two *toll receptors* (*PcToll5* and *PcToll6*) in response to white spot syndrome virus in the red swamp crayfish *Procambarus clarkii*. *Front. Physiol.* 9. doi: 10.3389/fphys.2018.00936

Huang, Y., Li, T., Jin, M., Yin, S., Hui, K.-M., and Ren, Q. (2017). Newly identified *PcToll4* regulates antimicrobial peptide expression in intestine of red swamp crayfish *Procambarus clarkii*. *Gene* 610, 140–147. doi: 10.1016/j.gene.2017.02.018

Hughes, A. L., and Piontkivska, H. (2008). Functional diversification of the toll-like receptor gene family. *Immunogenetics* 60, 249–256. doi: 10.1007/s00251-008-0283-5

IPCC (2014). Climate change 2014: Synthesis report. Contribution of working groups I, II and III to the fifth assessment report of the intergovernmental panel on climate change. Available at: https://www.ipcc.ch/site/assets/uploads/2018/02/AR5_SYR_FINAL_SPM.pdf.

Kawai, T., and Akira, S. (2010). The role of pattern-recognition receptors in innate immunity: update on toll-like receptors. *Nat. Immunol.* 11, 373–384. doi: 10.1038/ni.1863

Kumar, S., Stecher, G., and Tamura, K. (2016). MEGA7: molecular evolutionary genetics analysis version 7.0 for bigger datasets. *Mol. Biol. Evol.* 33, 1870–1874. doi: 10.1093/molbev/msw054

Lan, J. F., Zhao, L. J., Wei, S., Wang, Y., Lin, L., and Li, X. C. (2016a). PcToll2 positively regulates the expression of antimicrobial peptides by promoting PcATF4 translocation into the nucleus. *Fish Shellfish Immunol.* 58, 59–66. doi: 10.1016/j.fsi.2016.09.007

Lan, J., Wei, S., Wang, Y., Dai, Y., Tu, J., Zhao, L., et al. (2016b). *PcToll3* was involved in anti-vibrio response by regulating the expression of antimicrobial peptides in red swamp crayfish, *Procambarus clarkii*. *Fish Shellfish Immunol.* 57, 17–24. doi: 10.1016/j.fsi.2016.08.021

Letunic, I., Khedkar, S., and Bork, P. (2021). SMART: recent updates, new developments and status in 2020. *Nucleic Acids Res.* 49, 458–460. doi: 10.1093/nar/gkaa937

Li, Y., Chen, X., Lin, F., Chen, Q., Ma, Y., and Liu, H. (2017). *CqToll* participates in antiviral response against white spot syndrome virus *via* induction of anti-lipopolysaccharide factor in red claw crayfish *Cherax quadricarinatus*. *Dev. Comp. Immunol.* 74, 217–226. doi: 10.1016/j.dci.2017.04.020

Li, C., Wang, S., and He, J. (2019). The two NF-κB pathways regulating bacterial and WSSV infection of shrimp. *Front. Immunol.* 10. doi: 10.3389/fimmu.2019.01785

Li, W., Liu, Y., Lun, J., He, Y., and Tang, L. (2021). Heat stress inhibits TLR4-NF-κB and TLR4-TBK1 signaling pathways in broilers infected with Salmonella Typhimurium. *Int. J. Biometeorol.* 65, 1895–1903. doi: 10.1007/s00484-021-02146-5

Li, H., Yin, B., Wang, S., Fu, Q., Xiao, B., Lü, K., et al. (2018). RNAi screening identifies a new toll from shrimp *Litopenaeus vannamei* that restricts WSSV infection through activating dorsal to induce antimicrobial peptides. *PloS Pathog.* 14, e1007109. doi: 10.1371/journal.ppat.1007109

Liu, Q., Xu, D., Jiang, S., Huang, J., Zhou, F., Yang, Q., et al. (2018). *Toll-receptor 9* gene in the black tiger shrimp (*Penaeus monodon*) induced the activation of the TLR-NF-κB signaling pathway. *Gene* 639, 27–33. doi: 10.1016/j.gene.2017.09.060

Ma, K. Y., Qin, J., Lin, C. W., Chan, T. Y., Ng, P. K. L., Chu, K. H., et al. (2019). Phylogenomic analyses of brachyuran crabs support early divergence of primary freshwater crabs. *Mol. Phylogenet. Evol.* 135, 62–66. doi: 10.1016/j.ympev.2019.02.001

Macusi, E. D., Estor, D. E. P., Borazon, E. Q., Clapano, M. B., and Santos, M. D. (2022). Environmental and socioeconomic impacts of shrimp farming in the Philippines: a critical analysis using PRISMA. *Sustainability* 14, 2977. doi: 10.3390/su14052977

Mekata, T., Kono, T., Yoshida, T., Sakai, M., and Itami, T. (2008). Identification of cDNA encoding toll receptor, *MjToll* gene from kuruma shrimp, *Marsupenaeus japonicus*. *Fish Shellfish Immunol.* 24, 122–133. doi: 10.1016/j.fsi.2007.10.006

Miest, J. J., Politis, S. N., Adamek, M., Tomkiewicz, J., and Butts, I. A. E. (2019). Molecular ontogeny of larval immunity in European eel at increasing temperatures. *Fish Shellfish Immunol.* 87, 105–119. doi: 10.1016/j.fsi.2018.12.048

Nusslein-Volhard, C., Lohs-Schardin, M., Sander, K., and Christoph, C. (1980). A droso-ventral shift of embryonic primordial in a new maternal-effect mutant of *Drosophila*. *Nature* 283, 474–476. doi: 10.1038/283474a0

Ooi, J. Y. (2001). The *Drosophila* toll-9 activates a constitutive antimicrobial defense. *EMBO Rep.* 3, 82–87. doi: 10.1093/embo-reports/kvf004

Piamsomboon, P., Inchaisri, C., and Wongtavatchai, J. (2016). Climate factors influence the occurrence of white spot disease in cultured penaeid shrimp in chanthaburi province, Thailand. *Aquac. Environ. Interact.* 8, 331–337. doi: 10.3354/aei00176

Rambaut, A., Drummond, A. J., Xie, D., Baele, G., and Suchard, M. A. (2018). Posterior summarization in Bayesian phylogenetics using tracer 1.7. *Syst. Biol.* 67, 901–904. doi: 10.1093/sysbio/syy032

Roach, J. C., Glusman, G., Rowen, L., Kaur, A., Purcell, M. K., Smith, K. D., et al. (2005). The evolution of vertebrate toll-like receptors. *Proc. Natl. Acad. Sci. U. S. A.* 102, 9577–9582. doi: 10.1073/pnas.0502272102

Savitha, S. T., Kumar, V., Amitha, J. P., Sejian, V., Bagath, M., Krishnan, G., et al. (2021). Comparative assessment of thermo-tolerance between indigenous osmanabadi and Salem black goat breeds based on expression patterns of different intracellular *toll-like receptor* genes during exposure to summer heat stress. *Biol. Rhythm. Res.* 52, 127–135. doi: 10.1080/09291016.2019.1592350

Shen, C., Tang, D., Bai, Y., Luo, Y., Wu, L., Zhang, Y., et al. (2021). Comparative transcriptome analysis of the gills of *Procambarus clarkii* provide novel insights into the response mechanism of ammonia stress tolerance. *Mol. Biol. Rep.* 48, 2611–2618. doi: 10.1007/s11033-021-06315-y

Srisuk, C., Longyant, S., Senapin, S., Sithigorngul, P., and Chaivisuthangkura, P. (2014). Molecular cloning and characterization of a *Toll receptor* gene from *Macrobrachium rosenbergii*. *Fish Shellfish Immunol.* 36, 552–562. doi: 10.1016/j.fsi.2013.12.025

Sun, Y., Li, F., and Xiang, J. (2013). Analysis on the dynamic changes of the amount of WSSV in Chinese shrimp *Fenneropenaeus chinensis* during infection. *Aquaculture* 376-379, 124–132. doi: 10.1016/j.aquaculture.2012.11.014

Sun, X., and Zhang, S. (2022). Exosomes from WSSV-infected shrimp contain viral components that mediate virus infection. *J. Gen. Virol.* 103, 1776. doi: 10.1099/jgv.0.001776

Swift, M. L. (1997). GraphPad prism, data analysis, and scientific graphing. *J. Chem. Inf. Comp. Sci.* 37, 411–412. doi: 10.1021/ci960402j

Vidya, R., Paria, A., Deepika, A., Sreedharan, K., Makesh, M., Purushothaman, C. S., et al. (2014). Toll-like receptor of mud crab, *Scylla serrata*: molecular characterization, ontogeny and functional expression analysis following ligand exposure, and bacterial and viral infections. *Mol. Biol. Rep.* 41, 6865–6877. doi: 10.1007/s11033-014-3572-0

Visser, M., Zubakov, D., Ballantyne, K. N., and Kayser, M. (2011). mRNA-based skin identification for forensic applications. *Int. J. Legal. Med.* 125, 253–263. doi: 10.1007/s00414-010-0545-2

Wan, H., Mu, S., Baohua, D., Guo, S., and Kang, X. (2022). Genome-wide investigation of *toll-like receptor* genes (*TLRs*) in *Procambarus clarkia* and their expression pattern in response to black may disease. *Fish Shellfish Immunol.* 131, 775–784. doi: 10.1016/j.fsi.2022.10.066

Wang, Z., Chen, Y., Dai, Y., Tan, J., Huang, Y., Lan, J., et al. (2015). A novel vertebrates toll-like receptor counterpart regulating the anti-microbial peptides expression in the freshwater crayfish, *Procambarus clarkii*. *Fish Shellfish Immunol.* 43, 219–229. doi: 10.1016/j.fsi.2014.12.038

Wang, Z., Tang, D., Guo, H., Shen, C., Wu, L., and Luo, Y. (2020). Evolution of digestive enzyme genes associated with dietary diversity of crabs. *Genetica* 148, 87–99. doi: 10.1007/s10709-020-00090-7

Wang, Z., Tang, D., Shen, C., and Wu, L. (2022). Identification of genes involved in digestion from transcriptome of *Parasesarma pictum* and *Parasesarma affine* hepatopancreas. *Thalassas: Int. J. Mar. Sci.* 38, 93–101. doi: 10.1007/s41208-021-00296-2

Wang, Q., Wang, J., Wu, Q., Xu, X., Wang, P., and Wang, Z. (2021). Insights into the evolution of brachyura (Crustacea: decapoda) from mitochondrial sequences and gene order rearrangements. *Int. J. Biol. Macromol.* 170, 717–727. doi: 10.1016/j.ijbiomac.2020.12.210

Wu, L., Tang, D., Shen, C., Bai, Y., Jiang, K., Yu, Q., et al. (2021). Comparative transcriptome analysis of the gills of *Cardisoma armatum* provides novel insights into the terrestrial adaptive related mechanism of air exposure stress. *Genomics* 113, 1193–1202. doi: 10.1016/j.ygeno.2021.03.010

Xing, Q., Liao, H., Xun, X., Wang, J., Zhang, Z., Yang, Z., et al. (2017). Genome-wide identification, characterization and expression analyses of *TLRs* in yesso scallop (*Patinopecten yessoensis*) provide insight into the disparity of responses to acidifying exposure in bivalves. *Fish Shellfish Immunol.* 68, 280–288. doi: 10.1016/j.fsi.2017.07.020

Yang, Z. (2007). PAML 4: phylogenetic analysis by maximum likelihood. *Mol. Biol. Evol.* 24, 1586–1591. doi: 10.1093/molbev/msm088

Yang, Z., and Nielsen, R. (2000). Estimating synonymous and nonsynonymous substitution rates under realistic evolutionary models. *Mol. Biol. Evol.* 17, 32–43. doi: 10.1093/oxfordjournals.molbev.a026236

Yang, C., Zhang, J., Li, F., Ma, H., Zhang, Q., Jose-Priya, T. A., et al. (2008). A toll receptor from Chinese shrimp *Fenneropenaeus chinensis* is responsive to *Vibrio anguillarum* infection. *Fish Shellfish Immunol.* 24, 564–574. doi: 10.1016/j.fsi.2007.12.012

Zhang, J., Lü, J., Liu, P., Li, J., Wang, Z., and Zhang, X. (2018). Cloning of *Toll4* in *Portunus trituberculatus* and its expression in responding to pathogenic infection and low salinity stress. *Prog. Fishery Sci.* 39, 146–155. doi: 10.19663/J.ISSN2095-9869.20170307001

Zheng, J., Wang, P., Mao, Y., Su, Y., and Wang, J. (2020). Full-length transcriptome analysis provides new insights into the innate immune system of *Marsupenaeus japonicus*. *Fish Shellfish Immunol.* 106, 283–295. doi: 10.1016/j.fsi.2020.07.018

Zhou, X., Sun, F., Xu, S., Fan, G., Zhu, K., Liu, X., et al. (2013). Baiji genomes reveal low genetic variability and new insights into secondary aquatic adaptations. *Nat. Commun.* 4, 2708. doi: 10.1038/ncomms3708

Zhu, S., Yan, X., Shen, C., Wu, L., Tang, D., Wang, Y., et al. (2022). Transcriptome analysis of the gills of *Eriocheir sinensis* provide novel insights into the molecular mechanisms of the pH stress response. *Gene* 833, 146588. doi: 10.1016/j.gene.2022.146588